

# Planetary Gamma-Ray Spectroscopy of the Surface of Comet

J. Brueckner<sup>1</sup>, P. Domin<sup>2</sup>, and J. Masarik<sup>1,2</sup>

<sup>1</sup>Max-Planck-Institut f. Chemie, Abt. Kosmochemie, Postfach 3060, D-550 20 Mainz, Germany

<sup>2</sup>Department of Nuclear Physics, Faculty of Mathematics and Physics, Comenius University, Mlynska dolina F/2, SK-842 15 Bratislava, Slovakia

**Abstract:** To investigate the basic questions on the origin and evolution of comets and also solar system the data about the chemical composition of cometary nuclei are necessary. Gamma rays emitted from the cometary nucleus can be measured by a gamma-ray spectrometer on board an orbiting spacecraft. Flux of gamma rays emitted from the comet due to the interactions of cosmic ray particles with its surface was simulated using the Monte Carlo codes describing involved nuclear reactions.

## 1. Introduction

To approach basic scientific questions on the origin and evolution of comets one needs data on its elemental composition. The determination of the elemental composition of various celestial objects allows important constraints to be placed on its origin and evolution. The exploration of these objects must be carried out largely by remote observational techniques. At the present time, a variety of passive and active remote sensing techniques is available, and they can provide much of the needed information. The most commonly applied technique is passive remote sensing, in which the source of radiation is supplied from outside.

The comet is permanently bombarded by energetic galactic cosmic rays (GCR). They induce nuclear reactions leading to compositionally characteristic products. Among them are  $\gamma$  rays that can be measured by a  $\gamma$ -ray spectrometer on board an orbiting spacecraft. These  $\gamma$  rays can be used for the construction of global geochemical maps of the top few tens of centimeters of the surface [1]. Planetary gamma ray spectrometry was proposed around 1960 [2,3], but successful space missions with such instruments have been very rare.

Most theories about comets assume that they are pristine planetesimals that formed in the postulated Oort cloud in the Kuiper belt during an early period of the solar system. Recent observations of the Hubble Space telescope seem to confirm the existence of objects in the Kuiper belt. This implies that comets are the least differentiated bodies of the solar system, they accreted in the low-gravity fields, and existed for most of their lifetime in an extremely cold environment. This makes them very interesting from the point of view of understanding very early stages of our solar system formation.

In order to maximize the chance of success of future space missions to comets such as Rosetta mission, reliable modeling is needed. For the interpretation of measured  $\gamma$  ray fluxes in terms of the elemental composition of a planet's surface, a precise and accurate simulation of the production and transport phenomena is required. Studies of the influence of various parameters on  $\gamma$  ray fluxes from the cometary nucleus required

detailed numerical simulations that can only be achieved with physical models. We present here the results of simulations with such a model based on Los Alamos Code System (LCS). The influence of chemical composition and possible layered structure of the comet on  $\gamma$  ray fluxes were studied in details. Contributions to the background from the material surrounding detector and from neutrons emitted from radioactive heating unit were also investigated.

## 2. Sources of Gamma Rays

Gamma rays emitted from the cometary surface originate from several processes [1,4]. The  $\gamma$ -rays of interest for geochemical mapping arise from nuclear transitions between well-defined states and hence have unique, sharply defined energies. They are scattered or absorbed in the surface layer with a probability dependent on energy. The rays reaching an orbiting spectrometer originate mainly in the upper 50 cm or less of the surface.

There are two principal ways for formation of excited levels in nuclei in planetary surfaces: the decay of radioactive isotopes and excitation by cosmic-ray particles. The naturally radioactive elements (e. g. Th, K, and U) emit some  $\gamma$  ray in the course of their decay chains. These  $\gamma$  rays are emitted at a rate proportional to the elemental concentration. Fluxes of these  $\gamma$ -ray lines are relatively easy to calculate because they usually require only basic nuclear parameters [1].

The second source of  $\gamma$ -ray lines is the interaction of cosmic rays with planetary material. This source is very complicated, because involved are particles from wide energy range (from the high-energy, tens of GeV, primary GCR to thermal neutrons with less than an eV of energy). GCR particles interact in a planet to produce copious amounts of secondary particles, especially neutrons and pions. These primary and secondary GCR particles react with the nuclei in the planet by a variety of reactions to make  $\gamma$  rays. Most  $\gamma$  rays originate from two processes, both involving interactions by secondary neutrons. The first is neutron inelastic scattering, where a fast neutron ( $E_n$  1-15 MeV) raises the target nucleus to an excited state with several MeV of energy and this excited state de-excites by  $\gamma$ -ray emission. The second is thermal or epithermal neutron capture. In this case the excited nucleus typically has an energy of  $\sim 8$  MeV, which is dissipated in a cascade of  $\gamma$  rays. The huge energy range of the particles that participate in reactions leading to  $\gamma$ -ray production requires a very complex nuclear model for the simulation of relevant processes.

## 3. LCS Model for Calculation of Gamma-Ray Fluxes

In our model, the fluxes of particles inducing nuclear reactions in which  $\gamma$ -rays are produced are calculated using LCS, the Los Alamos LAHET Code System [5,6], which is a general-purpose, continuous-energy, generalized-3-dimensional-geometry, time-dependent, off-line-coupled, Monte Carlo computer code system that treats the relevant physical processes of particle production and transport. Individual codes in the system

treat all interactions of the considered particles within a specified energy range, and particles with energies outside this range are stored in “history” files, which are used as source input files for other LCS modules. The high-energy part of neutron interactions and all interactions of heavy ions, protons, mesons, muons, and other elementary particles are simulated by the Los Alamos version of the High-Energy Transport Code (HETC) [4]. Neutrons with energies below a cutoff value are written together with their kinematical parameters into a neutron file, which is the input file for the Monte Carlo N-particle (MCNP) code [7]. This code transports neutrons down to thermal energies. LCS, its tests, the basics of the built-in physical model, and its adaptation to planetary applications are described elsewhere [8], and therefore only the information most important for the  $\gamma$ -ray flux calculations is given here.

LCS is used to simulate the processes related to the production of  $\gamma$  rays emerging from inelastic scattering or neutron capture. The model for the calculation of  $\gamma$ -ray line fluxes from the decay of naturally radioactive elements is not subject of present study and was published earlier [9]. The GCR proton spectrum was used as input for the LAHET code, which tracks secondary protons and neutrons from intra- and inter-nuclear cascade and evaporation. Proton histories are followed down to an energy of 1 MeV, whereas neutrons below 15 MeV and  $\pi^0$  mesons are stored in history files for further transport with MCNP. The cutoff energy of 15 MeV was chosen because the parameters used by LAHET are global averages for all nuclei that become questionable for some nuclei toward lower energies (mainly neutron elastic cross sections) and because the individual cross-section libraries for neutron production and transport used by MCNP become sparse toward higher energies.

While LCS can calculate  $\gamma$ -ray line fluxes as one of its outputs, we used this option only for rates of neutron-capture reactions, where the MCNP code is coupled to very massive libraries that contain state-of-the-art neutron-capture cross sections, and for estimations of the  $\gamma$ -ray continuum. In all other cases we used LCS only to calculate the fluxes of particles that lead to  $\gamma$ -ray production.

Assuming isotropic irradiation of a sphere with radius  $R$  by GCR particles, the photon production rate of nonelastic-scattering  $\gamma$  ray  $j$  at a depth  $r$  is

$$P_j(r) = \sum_i N_i \sum_k \sigma_{ijk}(E_k) J_k(E_k, r) dE_k \quad (1)$$

where  $N_i$  is the number of atoms for target element  $i$  per kg material in the sample,  $\sigma_{ijk}$  is the cross section for the production of  $\gamma$  ray  $j$  from target element  $i$  by particles of type  $k$  with energy  $E_k$ , and  $J_k(E_k, r)$  is the total (primary plus secondary) flux of particles of type  $k$  with energy  $E_k$  at location  $D$  inside the irradiated body. This expression is very similar to the one in [8] that has been successfully used for the calculation of cosmogenic nuclide production in meteorites. As stated earlier, the particle fluxes  $J_k(E_k, r)$  are calculated using LCS. The cross sections  $\sigma_{ijk}$  were ones evaluated from many measurements and used in earlier  $\gamma$ -ray-flux calculations by [1,9,10]. There have been some cross sections measured for the production of nonelastic-scattering  $\gamma$  rays since then, but few reactions would have cross sections much different from those used here.

As in almost all applications of gamma-ray spectroscopy, only  $\gamma$  rays that arrive at the detector without changing energy are used for mapping elements, so we concentrated our attention on them.

## 4. Calculational Procedures

### 4.1 Model of cometary nucleus

In our calculations, Comet was modeled as a sphere with the radius  $R = 2$  km. Elemental chemical composition of the nucleus is subject of proposed investigations, however based on the present state of knowledge of comets, their chemical composition was simulated as mixture of rocky component and different ices. The chemical composition of the rocky component was in accordance with former investigations e. g. [11] taken to be equivalent to type I carbonaceous chondrites. The icy component consisted from  $\text{CO}_2$ ,  $\text{H}_2\text{O}$  and  $\text{HCN}$ . The weight fractions of rocky and icy components varied in our model compositions and also the weight fractions of different ices varied in the simulations. As result of these variations we got 8 basic chemical compositions that are listed in Table 1. For each rocky to ice ratio, the composition was normalized in such a way that the sum of the weight fractions of all elements present in a particular composition was 1.0. A homogenous distribution of all elements in the cometary nucleus was assumed in first set of simulations. As most of the models prefer layered structure of cometary nucleus, also the layered structure was simulated. For those cases the nucleus of comet was modeled as the mixture of dust and ice of chemical composition 5 covered with rocky component of chemical composition 1

Because the particle production and equilibrium spectra are strongly depth-dependent, the cometary sphere was divided into concentric shells of varying thickness, with many layers near the surface and fewer layers at greater depths. We used a density of  $1 \text{ g cm}^{-3}$  for the cometary surface. The thickness of a shell resulted from the compromise between two opposite requirements: the minimization of statistical errors in the calculations, which are approximately inversely proportional to the shell thickness, and the investigation of the depth dependence of the particle fluxes, which can be more precisely described by splitting the investigated body into finer shells. We defined a few layers with a thickness of 1 mm near the surface, and going deeper the thickness of the layers gradually increased to 4 cm at depths 30 cm below the surface. The transport of rays assumed that the ray was produced at a depth  $x$  in the middle of each layer.

### 4.2 Gamma Rays from Natural Radioactivity

The rays made by the decay of the naturally radioactive elements of potassium  $^{40}\text{K}$ , thorium  $^{232}\text{Th}$ , uranium (mainly  $^{238}\text{U}$ ), and the daughter isotopes of U and Th are important in planetary studies. Details on the production of these rays and their transport to the surface assuming a constant concentration with depth are described in [1] and [9]. They were not subject of this study.

### 4.3 Galactic Cosmic Rays

The simulation of particle production and transport processes begins with a choice of the primary particle type and its energy. The comet surface was modeled as a sphere irradiated by a homogenous, isotropic particle flux. Paper [9] gave a list of  $\gamma$  rays resulting from nuclear reactions induced by solar-cosmic-ray (SCR) particles striking the Moon. Such sources of  $\gamma$  rays are much less important for comets. Because the long-term average flux of SCR particles in the solar system varies roughly inversely with the square to cube of the distance from the Sun [12]; their fluxes at comet are only a few % of those at the Moon.

Taking into account the accuracy of many parameters used in the calculations, we considered only GCR as input particles.

Galactic cosmic rays consist of ~87% protons, ~12% alpha particles, and ~1% heavier nuclei with atomic numbers from 3 to ~90 [13]. If energies are expressed as per-nucleon values, the spectral distribution of the heavier particles is quite similar to that for protons. The GCR particles originate far from the solar system, and during their diffusion and transport to the solar system they are influenced by many interactions that lead to spatial and time variability of their fluxes. Among these influences, probably the dominant is solar modulation, which is taken into account in the expression for the differential GCR proton flux. According to [14], the differential spectra of primary protons can be described by

$$J(E_p, \_) = C_p \frac{E_p (E_p + 2m_p c^2) (E_p + \_ + \_)^{-2.5}}{(E_p + \_) (E_p + 2m_p c^2 + \_)} \quad (2)$$

where  $\_ = 780 \exp(-2.5 \times 10^{-4} E_p)$ ,  $E_p$  is the proton's kinetic energy,  $\_$  is the parameter that takes into account the modulation effect due to solar activity,  $m_p$  is the mass of the proton,  $c$  is the velocity of light,  $m_p c^2$  is 938 MeV, and  $C_p = 1.244 \times 10^6 \text{ cm}^{-2} \text{ s}^{-1} \text{ MeV}^{-1}$  is the normalization factor. For GCR alpha particles, analogous formulae hold with slightly different parameters [15]. In our calculations we used only one value of the modulation parameter,  $\_ = 550 \text{ MeV}$ , which is very close to the one used for describing the GCR flux averaged over a solar cycle [16].

The percentage of alpha particles in the primary GCR spectrum is fairly high (the ratio of alpha particles to protons is 0.14), and therefore they have to be considered in every precise Monte Carlo simulation. The contribution of alpha particles is therefore included in our final results by normalizing the proton calculations by a scaling factor, which was found on the basis of previous [9] calculations to be 1.4. The results presented in this paper are based on calculations in which we simulated the irradiation using 100,000 primary GCR protons with energies  $0.01 < E < 20 \text{ GeV}$  and the spectral distribution given above.

#### 4.4 Gamma-Ray Production and Transport}

For  $\gamma$  rays emerging from neutron capture and neutron nonelastic-scattering reactions, the source term, that is, the rate at which  $\gamma$  rays are produced, is calculated according to Eq. (1). As the flux of particles that induce nuclear reactions in which  $\gamma$  rays are produced

is depth dependent, the source term is usually also depth dependent (see Figures 1 and 2 for the source terms for the major  $\gamma$  rays from reactions of thermal and fast neutrons on Fe).

In our calculations we are not concerned with scattered photons, but only with the photons that undergo no interactions before they reach the detector. For planetary  $\gamma$  rays, coherent scattering is also ignored. We calculated the flux of such  $\gamma$  rays, that is defined as the intensity of photons reaching a unit-area isotropic detector above the planetary surface. Once the source term is known, the transport of the  $\gamma$  rays from their point of creation to the detector must be considered.

An important parameter in calculating the flux of  $\gamma$  rays that escape from a planet with their original energy is the exponential mass attenuation coefficient,  $\mu$ , in each medium through which the  $\gamma$  rays pass. The  $\gamma$ -ray attenuation coefficients are functions of the  $\gamma$ -ray's energy and of the medium's composition, and therefore they were calculated for each  $\gamma$ -ray line and each composition used in the simulations.

The calculation of the  $\gamma$ -ray flux reaching the cometary surface and a detector on the surface was done similarly to that by [1,9,17]. Our case is different in two senses presence of layered structures in some models of cometary nucleus and finite dimensions of investigated object (sphere with radius  $R = 2$  km). In general, if the detector D is on the cometary surface (Fig. 3), the flux F of a  $\gamma$  ray entering the isotropis is calculated as

$$F(r) = \int_0^{\pi/2} \sin \theta \, d\theta \int_0^r \frac{P(r)}{4} \frac{r}{x_1 + x_2} e^{-\mu_1 x_1} e^{-\mu_2 x_2} \quad (3)$$

where  $\theta$  is the angle between the normal to the surface and the line connecting the point of  $\gamma$ -ray creation with the detector;  $x_1 + x_2$  is the distance of the detector from the  $\gamma$ -ray source,  $\mu_1$  and  $\mu_2$  are attenuation coefficient for particular  $\gamma$  ray in the layer 1 and 2 respectively

## 5. Results and discussion

In this part we present the results of gamma-ray flux calculations, convert them to the counting rate and show how precisely the chemical composition of cometary surface can be determined from them. We would like to stress that these values were calculated entirely; no scaling of experimental data was applied. The production of  $\gamma$  rays was calculated using the above described LCS code system and experimental or evaluated cross-section data.  $\gamma$  rays were transported from the point of their creation to the detector using the code written for this purpose. Both these codes were used also in calculations of the background of the  $\gamma$ -ray spectrum. The Monte Carlo code ACCEPT [18] was used for the determination of internal efficiencies of the detector the germanium detector.

In Table 2 are presented results of these calculations for homogenous comet of bulk chemical composition #5 (Tab. 1). The errors listed in the last three columns of this table represent the errors in the determination of the concentration of particular element with preset time for accumulation of  $\gamma$ -ray spectrum. The error is derived from the peak area of the line and the underlying background for a given counting time. Characteristic strongest  $\gamma$ -ray lines that show no sign for large interferences in realistic prompt  $\gamma$ -ray spectra were selected for neutron inelastic and neutron capture reactions, each (Tab. 2). The lines are

ordered by counting time, so showing a kind of sensitivity for each element. For the chemical composition #5 (Tab. 1), the following elements can be determined with decreasing precision: H, Fe, O, Mg, Si, C, S, Ni, Na, and N. Of course, this order depends on detection sensitivity and concentration of each element. If large counting times are available, the resulting errors are accordingly shorter. Table 3 and 4 contain equivalent results for the comets with layered structure of their nucleus. The thickness of the surface layer was 0.5 and 20 g cm<sup>-2</sup>, respectively. Since these three investigated cases produce unique gamma-ray signals, the three models of cometary nucleus can be clearly distinguished. In the case of the mission to a comet, one receives  $\gamma$ -ray spectra emitted by surface area of unknown composition. The measured  $\gamma$ -ray flux will be compared with the fluxes obtained from the simulated cases of known chemical composition. Using some inversion procedure, a corresponding chemical composition that fits the measured  $\gamma$ -ray spectra will be derived.

## Conclusions

We have shown that for a future missions to comet, a  $\gamma$ -ray spectrometer will be an invaluable instrument to provide data on elemental chemical composition of the surface. Monte Carlo simulations were carried out for various models of cometary nucleus. The simulations show that: (1) the  $\gamma$ -ray data allow to distinguish various types of the compositions, (2) the layered structure of the comet can be distinguished from homogenous case and also the thickness of the layer can be determined with restricted accuracy. These data can be used to derive the constraints for models on origin and evolution of comets.

## Acknowledgment

We thank our colleagues for their comments and encouragement. One author (J.M.) thanks for the support of his work from MPI Mianz, especially from Prof. H. Waenke, during his stay at the Institute. On this special occasion we (J.M. and P.D.) would like to express our thanks also to our teacher and friend M. Chudy, for his interest and help in our work.

## References

- [1] R.C. Reedy, J. R. Arnold, and J. I. Trombka: *J. Geophys. Res.* 78 (1973) 5847.
- [2] J.R. Arnold et al.: *J. Geophys. Res.* 67 (1962) 4870.
- [3] M.A. Van Dilla et al.: *IRE Trans. Nucl. Sci.* NS-9 (1962) 405.
- [4] T.W. Armstrong: *J. Geophys. Res.*, 77 (1972) 524.
- [5] R.E. Prael and H. Lichtenstein: *User guide to LCS. The LAHET Code System*, LANL report LA-UR-89-3014 (1989) 76 pp.

- [6] R.E. Prael: *Nuclear Data Evaluation Methodology*, edited by C. L. Dunford, World Scientific, Singapore, (1993) 525.
- [7] J.F. Briesmeister: *MCNP - A general Monte Carlo N-particle transport code, version 4A*, LANL report LA-12625-M (1993) 693 pp.
- [8] J. Masarik and R. C. Reedy: *Geochim. Cosmochim. Acta* 58 (1994) 5307.
- [9] R.C. Reedy: *Proc. Lunar Planet. Sci. Conf.* 9 (1978) 2961.
- [10] J. Masarik and R. C. Reedy: *J.Geophys. Res.* 101 (1996) 18,1891.
- [11] E.K. Jessberger, A. Christoforidis, and J. Kissel: *Nature* 332 (1988) 691.
- [12] M.A. Shea et al.: *Interplanetary Particle Environment, JPL Publication 88-28* edited by J. Feynman and S. Gabriel, Jet Propulsion Laboratory, Pasadena, (1988) 3.
- [13] J.A. Simpson: *Annu. Rev. Nucl. Part. Sci.* (1983) 323.
- [14] G.C. Castagnoli and D. Lal: *Radiocarbon* 22 1980 (133).
- [15] D. Lal: *Solar-terrestrial relationship and the Earth environment in the last millennia* edited by G. C. Castagnoli, North-Holland, Amsterdam, (1988) 216.
- [16] R.C. Reedy: *J. Geophys. Res.* 92 (1987) E697.
- [17] J. Brueckner and J. Masarik: *Planet. Space Sci.* (1997) 39.
- [18] J. A. Helbleih and T. A. Mehlborn: *ITS: the integrated TIGER series of coupled electron photon Monte Carlo transport codes*, Sandia Nat. Lab. Preprint SAND 84-0573 (1984) 99pp.



## Figure Caption

- Fig. 1. Calculated depth profile of the production rate for making the 7.6313 MeV inelastic scattering  $\gamma$  ray in the layered comet.
- Fig. 2. Calculated depth profile of the production rate for making the 0.8467 MeV neutron-capture  $\gamma$  ray in the layered comet.
- Fig. 3. Geometry assumed for  $\gamma$  ray production and transport for a detector (D) at the surface of comet. Dimensions are not to scale.

Table 1. Chemical compositions for which the  $\gamma$  ray fluxes were simulated. Composition 1 represents type I carbonaceous chondrites; in compositions 3-6 is rock to ice ratio 1 and varied is only fraction of different ices within the icy component.

Element	Chemical composition [in weight %]							
	1	2	3	4	5	6	7	8
H	1.51	2.49	3.27	3.37	3.46	3.55	4.43	5.02
C	3.50	6.81	13.19	11.65	10.11	8.57	13.42	15.40
N	-	1.30	7.77	5.18	2.59	-	3.89	4.66
O	47.0	53.42	51.77	55.80	59.84	63.88	66.26	70.12
Na	0.50	0.37	0.25	0.25	0.25	0.25	0.13	0.05
Mg	9.36	7.02	4.68	4.68	4.68	4.68	2.34	0.94
Al	0.82	0.61	0.41	0.41	0.41	0.41	0.21	0.08
Si	10.68	8.01	5.34	5.34	5.34	5.34	2.67	1.07
S	5.80	4.35	2.90	2.90	2.90	2.90	1.45	0.58
K	0.05	0.04	0.03	0.03	0.03	0.03	0.01	0.01
Ca	0.90	0.67	0.45	0.45	0.45	0.45	0.23	0.09
Ti	0.04	0.03	0.02	0.02	0.02	0.02	0.01	0.00
Co	0.27	0.20	0.14	0.14	0.14	0.14	0.07	0.03
Mn	0.18	0.13	0.09	0.09	0.09	0.09	0.05	0.02
Fe	18.30	13.72	9.15	9.15	9.15	9.15	4.58	1.83
Ni	1.08	0.81	0.54	0.54	0.54	0.54	0.27	0.11
Total	1.00	1.00	1.00	1.00	1.00	1.00	1.00	1.00

Table 2. Calculated  $\gamma$ -ray fluxes of  $\gamma$ -ray lines characteristic for an element (column El) and energy for homogenous comet composition #5 from Table 1. 'Error' are errors with which is the concentration of particular element present in the cometary nucleus determined using the  $\gamma$ -ray spectra accumulated during the preset counting times 10, 24 or 240 hours. Keys: I =  $\gamma$  ray produced in inelastic neutron reaction; C =  $\gamma$  ray produced in neutron capture reaction; Conc. = concentration of target element in the considered chemical composition; Int. Eff. = internal efficiency of the detector for the detection of  $\gamma$  ray of given energy.

El.	Energy [MeV]	Mode	Conc. [wt. %]	Int. Eff.	Flux [ rays cm <sup>-2</sup> min <sup>-1</sup> ]	Backg.	10 hours	24 hours	240 hours
							Error		
							[%]	[%]	[%]
H	2.2233	C	3.46	0.075	7.438	0.038	1.19	0.77	0.24
Fe	0.8467	I	9.15	0.181	0.426	0.105	4.77	3.08	0.97
O	6.1294	I	59.84	0.019	1.728	0.014	5.57	3.59	1.14
Mg	1.3686	I	4.68	0.117	0.333	0.063	7.04	4.54	1.44
Fe	7.6313	C	9.15	0.013	1.501	0.008	7.24	4.67	1.48
Si	1.7788	I	5.34	0.091	0.347	0.047	7.63	4.92	1.56
Fe	7.6457	C	9.15	0.013	1.377	0.008	7.65	4.94	1.56
O	4.4383	I	59.84	0.031	1.013	0.194	13.18	8.51	2.69
Fe	1.2383	I	9.15	0.126	0.120	0.067	16.27	10.5	3.32
C	4.4383	I	10.11	0.031	0.802	0.194	16.41	10.59	3.35
S	5.424	C	2.9	0.023	0.316	0.016	18.27	11.8	3.73
Si	3.5395	C	5.34	0.040	0.187	0.024	20.3	13.11	4.14
S	2.379	C	2.9	0.067	0.129	0.033	20.53	13.25	4.19
Si	4.934	C	5.34	0.028	0.216	0.017	21.64	13.97	4.42
Si	1.7789	I	5.34	0.091	0.092	0.047	24.27	15.67	4.95
Ni	8.999	C	0.54	0.009	0.249	0.005	31.81	20.53	6.49
Mg	1.3686	I	4.68	0.117	0.054	0.063	35.66	23.02	7.28
Si	1.3686	I	5.34	0.117	0.035	0.063	53.7	34.67	10.96
Mg	3.918	C	4.68	0.039	0.058	0.022	59.93	38.69	12.23
Na	1.3686	C	0.25	0.117	0.026	0.063	72.78	46.98	14.86
Na	0.4399	I	0.25	0.349	0.014	0.228	83.79	54.08	17.1
Fe	2.5231	I	9.15	0.062	0.027	0.029	90.26	58.26	18.42
N	5.2693	C	2.59	0.022	0.052	0.016	97.94	63.22	19.99
Fe	0.8467	I	9.15	0.181	0.016	0.105	98.09	63.31	20.02

Table 3. Calculated  $\gamma$ -ray fluxes of  $\gamma$ -ray lines characteristic for an element (column El) and energy for layered comet with layer thickness of 5 g cm<sup>-2</sup>. ‘Error’ are errors with which is the average concentration of particular element present in the cometary nucleus determined using the  $\gamma$ -ray spectra accumulated during the preset counting times 10, 24 or 240 hours. Keys: I =  $\gamma$  ray produced in inelastic neutron reaction; C =  $\gamma$  ray produced in neutron capture reaction; Conc.1 and 5 = concentration of target element in the surface and inner layer of the comet, respectively; Int. Eff. = internal efficiency of the detector for the detection of  $\gamma$  ray of given energy.

El.	Energy	Mode	Conc.1	Conc.# 5	Int. Eff.	Flux	Backg	10 hours	24 hours	240 hours
-----	--------	------	--------	-------------	--------------	------	-------	-------------	-------------	--------------

								Error		
	[MeV]		[%]	[%]				[%]	[%]	[%]
H	2.2233	C	1.51	3.46	0.075	7.413	0.038	1.19	0.77	0.24
Fe	0.8467	I	18.3	9.15	0.181	0.480	0.105	4.34	2.8	0.89
O	6.1294	I	47	59.84	0.019	1.777	0.014	5.47	3.53	1.12
Mg	1.3686	I	9.36	4.68	0.117	0.370	0.063	6.47	4.17	1.32
Si	1.7788	I	10.68	5.34	0.091	0.383	0.047	7.06	4.55	1.44
Fe	7.6313	C	18.3	9.15	0.013	1.521	0.008	7.18	4.63	1.47
Fe	7.6457	C	18.3	9.15	0.013	1.396	0.008	7.59	4.9	1.55
Si	3.5395	C	10.68	5.34	0.040	0.191	0.024	20	12.91	4.08
S	2.379	C	5.8	2.9	0.067	0.132	0.033	20.15	13	4.11
Si	4.934	C	10.68	5.34	0.028	0.220	0.017	21.36	13.79	4.36
Si	1.7789	I	10.68	5.34	0.091	0.101	0.047	22.11	14.27	4.51
Ni	8.999	C	1.08	0.54	0.009	0.252	0.005	31.47	20.31	6.42
Mg	1.3686	I	9.36	4.68	0.117	0.060	0.063	32.17	20.77	6.57
Si	1.3686	I	10.68	5.34	0.117	0.040	0.063	47.68	30.78	9.73
Mg	3.918	C	9.36	4.68	0.039	0.059	0.022	59	38.08	12.04
Na	1.3686	C	0.5	0.25	0.117	0.027	0.063	71.05	45.86	14.5
Na	0.4399	I	0.5	0.25	0.349	0.017	0.228	71.97	46.46	14.69
Fe	2.5231	I	18.3	9.15	0.062	0.030	0.029	82.42	53.2	16.82
Fe	0.8467	I	18.3	9.15	0.181	0.018	0.105	85.84	55.41	17.52
N	5.27	C	0	2.59	0.022	0.052	0.016	98.22	63.4	20.05

Table 4. Calculated  $\gamma$ -ray fluxes of  $\gamma$ -ray lines characteristic for an element (column El) and energy for layered comet with layer thickness of 20 g cm<sup>-2</sup>. ‘Error’ are errors with which is the average concentration of particular element present in the cometary nucleus determined using the  $\gamma$ -ray spectra accumulated during the preset counting times 10, 24 or 240 hours. Keys: I =  $\gamma$  ray produced in inelastic neutron reaction; C =  $\gamma$  ray produced in neutron capture reaction; Conc.1 and 5 = concentration of target element in the surface and inner layer of the comet, respectively; Int. Eff. = internal efficiency of the detector for the detection of  $\gamma$  ray of given energy.

El.	Energy	Mode	conc.# 1	conc.# 5	Int. Eff.	Flux	Backg	20 hours	24 hours	240 hours
	[MeV]		[%]	[%]		[1]	[2]	Error		
								[%]	[%]	[%]
H	2.2233	C	1.51	3.46	0.075	4.524	0.038	1.55	1	0.32
Fe	0.8467	I	18.3	9.15	0.181	1.182	0.105	2.27	1.47	0.46
Mg	1.3686	I	9.36	4.68	0.117	0.840	0.063	3.51	2.27	0.72
Si	1.7788	I	10.68	5.34	0.091	0.859	0.047	3.89	2.51	0.79
O	6.1294	I	47	59.84	0.019	1.737	0.014	5.55	3.58	1.13

Fe	7.6313	C	18.3	9.15	0.013	1.816	0.008	6.42	4.14	1.31
Fe	7.6457	C	18.3	9.15	0.013	1.666	0.008	6.78	4.37	1.38
Fe	1.2383	I	18.3	9.15	0.126	0.306	0.067	7.24	4.67	1.48
Si	1.7789	I	10.68	5.34	0.091	0.217	0.047	11.25	7.26	2.3
O	4.4383	I	47	59.84	0.031	0.962	0.194	13.84	8.93	2.82
S	5.424	C	5.8	2.9	0.023	0.403	0.016	14.92	9.63	3.04
S	2.379	C	5.8	2.9	0.067	0.179	0.033	15.36	9.91	3.13
Si	3.5395	C	10.68	5.34	0.040	0.245	0.024	16.09	10.38	3.28
Mg	1.3686	I	9.36	4.68	0.117	0.125	0.063	16.41	10.59	3.35
Si	4.934	C	10.68	5.34	0.028	0.274	0.017	17.68	11.42	3.61
C	4.4383	I	3.5	10.11	0.031	0.534	0.194	24.18	15.61	4.94
Si	1.3686	I	10.68	5.34	0.117	0.075	0.063	26.21	16.92	5.35
Ni	8.999	C	1.08	0.54	0.009	0.297	0.005	27.48	17.74	5.61
Na	0.4399	I	0.5	0.25	0.349	0.042	0.228	28.97	18.7	5.91
Fe	2.5231	I	18.3	9.15	0.062	0.063	0.029	40.08	25.87	8.18
Fe	0.8467	I	18.3	9.15	0.181	0.039	0.105	40.56	26.18	8.28
Mg	3.918	C	9.36	4.68	0.039	0.075	0.022	46.97	30.32	9.59
Na	1.3686	C	0.5	0.25	0.117	0.037	0.063	51.56	33.28	10.52
Si	2.2235	I	10.68	5.34	0.075	0.032	0.038	71.09	45.89	14.51

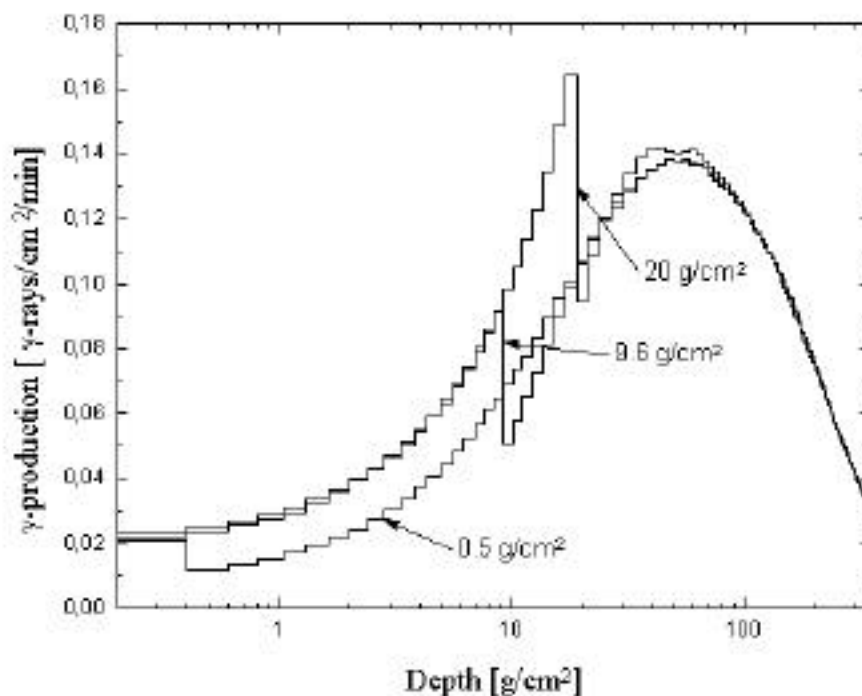


Fig.1

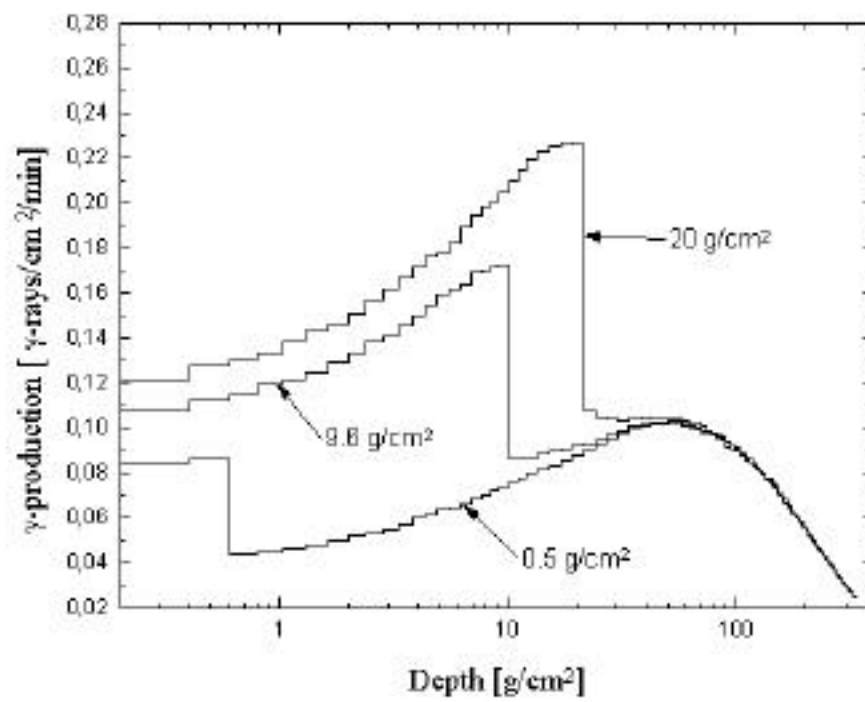


Fig. 2

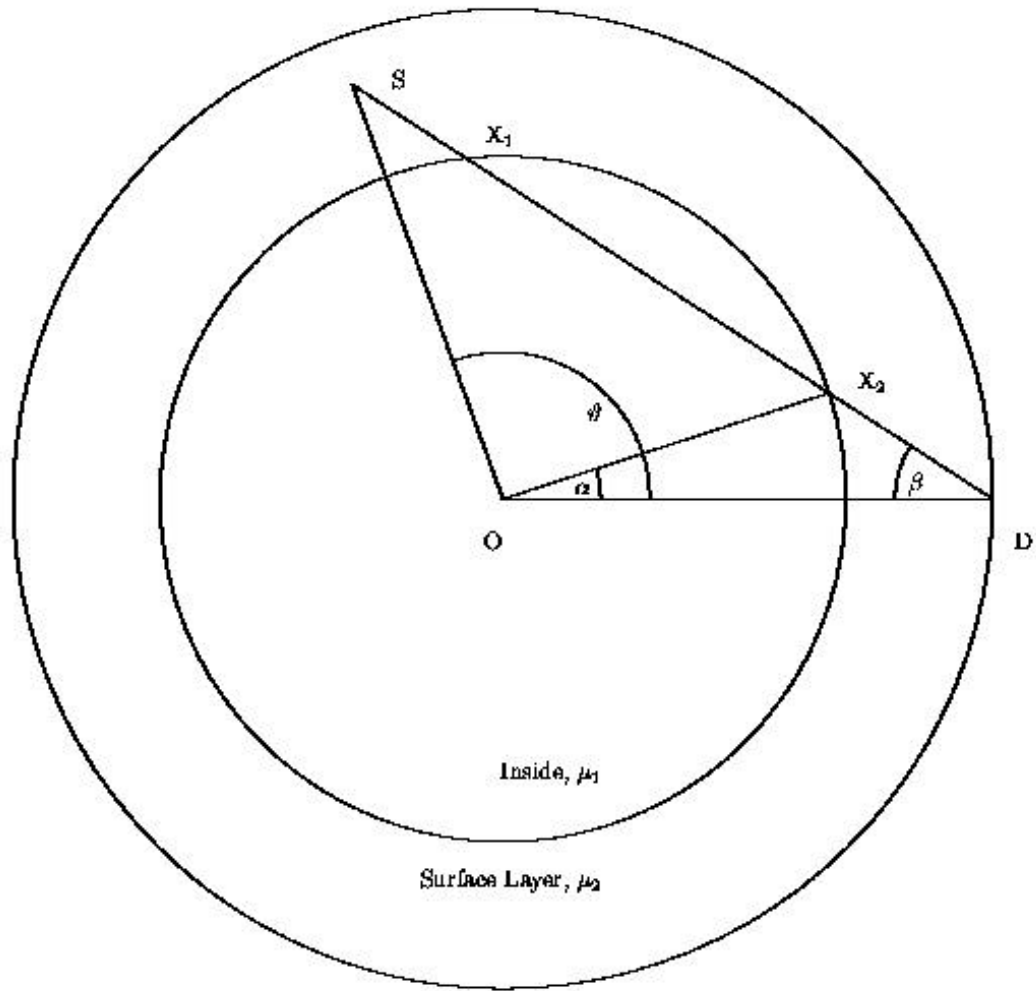


Fig.3